Transient Dynamical Problem for a Accreted Thermoelastic Parallelepiped

Alexander L. Levitin, Sergei A. Lychev, and Iusup N. Saifutdinov

***Abstract*—The discrete accretion is often realized in technological processes such as laser surfacing, gas-dynamic deposition, and vapor phase deposition. Mathematical modeling of the deformations and temperature fields arising in these processes allows one to optimize the technological processes and is a topical problem of mechanics of deformable body. In present paper an illustrative example an initial boundary-valued problem for thermoelastic growing parallelepiped is studied. Full coupling of mechanical and thermal fields as well as relaxing of the heat flux are taken into account. A closed form solution is constructed for a body under "smoothly rigid" heat-insulated fixation conditions for the stationary faces and the growing load-free face. The temperature field on the growing face is analyzed numerically for various accretion scenarios. An analysis of the temperature behavior on the growth boundary shows that, depending on the accretion rate, the boundary can be considered as an isothermal (for high values of the accretion rate) boundary or a boundary with variable effective temperature determined in the process of solving the problem.**

***Index Terms*—coupled thermoelasticity, micromechanics, growing bodies, discrete accretion, inconsistency.**

I. Statement of the Problem

THE thermomechanics of growing bodies studies the distributions of mechanical and thermal fields in quasistatic and dynamic processes that occur in the bodies whose composition varies in the process of deformation and heating. These types of accretion are often realized in technological processes such as laser surfacing, gas-dynamic deposition, and vapor phase deposition. Mathematical modeling of the deformations and temperature fields arising in these processes allows one to optimize the technological processes and is a topical problem of mechanics of deformable rigid body.

Mechanics of growing bodies studies the stress-strain state and dynamic processes in bodies whose composition varies in the process of deformation [1]–[7]. A discretely accreted body is represented as a finite family of bodies [6], [7]:

$$\mathfrak{B}_0 \subset \mathfrak{B}_1 \subset \mathfrak{B}_2 \subset \ldots \subset \mathfrak{B}_N. \tag{1}$$

The sequence (1) is associated with the sequence of numbers

$$0 < \tau_1 < \tau_2 < \ldots < \tau_N \tag{2}$$

Manuscript received March 14, 2014; revised March 31, 2014. This work was supported in part by the Russian Science Foundation under Grant 14-19-01280, Russian Foundation for Basic Research under Grants 12-08-01119-a, 12-08-01260-a, 14-01-00741-a, 13-01-92693-IND_a and by the Department of Energetics, Mechanical Engineering, Mechanics and Control Processes of the Russian Academy of Sciences under Program No. 12.

A.L. Levitin is with the Department of Modelling in Solid Mechanics, Institute for Problems in Mechanics, pr-t Vernadskogo 101, str. 1, Moscow, 119526 Russia (e-mail: alex_lev@ipmnet.ru)

S.A. Lychev is with the Department of Modelling in Solid Mechanics, Institute for Problems in Mechanics and Bauman Moscow State Technical University, Moscow, Russia (e-mail: lychevsa@mail.ru)

I.N. Saifutdinov is with "RSU-1", Samara (e-mail: jusufsay@gmail.com)

determining the accretion times, i.e., the times at which the parts $\mathfrak{B}_{k+1} \setminus \mathfrak{B}_k$, $k = 0, \ldots, N-1$ are added to the body. The sequences (1) and (2) together determine the body growth scenario. The strain, temperature, and velocity fields of the part $\mathfrak{B}_{k+1} \setminus \mathfrak{B}_k$ added at time τ_k are generally inconsistent with the fields of the body $\mathfrak{B}_k$. Therefore, the dynamic processes in the growing body vary by jump at the attachment times.

II. General Procedure

The process of dynamic discrete accretion can be modeled by successively solving the boundary value problems for the bodies $\mathfrak{B}_k$. Then the initial data for the step k ($k \geq 1$) are determined by the values of the corresponding fields at the final time moment of the step $k-1$ and by the values associated with the attached elements. Formally, the recursive sequence of problems in the linear approximation can be stated as follows:

$$\begin{gathered}
\forall \mathbf{x} \in \mathfrak{B}_0 \quad \mathcal{L}_0 \mathbf{y}_0 + \mathbf{f}^0 = \mathbf{0}, \\
\forall \mathbf{x} \in \partial\mathfrak{B}_0 \quad \mathcal{B}_0 \mathbf{y}_0 = \mathbf{0}, \quad \mathbf{y}_0\big|_{t=0} = \mathbf{y}_0^0, \quad \dot{\mathbf{y}}_0\big|_{t=0} = \mathbf{v}_0^0, \\
\ldots \\
\forall \mathbf{x} \in \mathfrak{B}_n \quad \mathcal{L}_n \mathbf{y}_n + \mathbf{f}_n^0 = \mathbf{0}, \\
\forall \mathbf{x} \in \partial\mathfrak{B}_n \quad \mathcal{B}_n \mathbf{y}_n = \mathbf{0}, \quad \mathbf{y}_n\big|_{t=\tau_n} = \mathbf{0}, \quad \dot{\mathbf{y}}_n\big|_{t=\tau_n} = \mathbf{v}_n^0, \\
\ldots \\
\mathbf{f}_n^0 = \mathbf{f}^0 + \begin{cases} \mathcal{L}_{n-1}\mathbf{y}_{n-1}\big|_{t=\tau_n}, & \mathbf{x} \in \mathfrak{B}_{n-1}, \\ 0, & \mathbf{x} \in \mathfrak{B}_n \setminus \mathfrak{B}_{n-1}, \end{cases} \\
\mathbf{v}_n^0 = \begin{cases} \dot{\mathbf{y}}_{n-1}\big|_{t=\tau_n}, & \mathbf{x} \in \mathfrak{B}_{n-1}, \\ \mathbf{v}^0, & \mathbf{x} \in \mathfrak{B}_n \setminus \mathfrak{B}_{n-1}. \end{cases}
\end{gathered}$$

Here $\mathcal{L}_0, \ldots, \mathcal{L}_N$ are differential operators determined by the same differential operation (the field equations) but in different domains, $\mathcal{B}_0, \ldots, \mathcal{B}_N$ are operators of boundary conditions, $\mathbf{f}^0$ are external force and thermal fields, $\mathbf{v}^0$ are the velocities associated with the attached elements, and $\mathbf{y}_0, \ldots, \mathbf{y}_N$ are increments of the displacement and temperature fields with respect to the beginning of the step. The dot denotes the derivative with respect to time, and $\mathbf{y}_0^0$, $\mathbf{v}_0^0$ are the initial data for the first step.

The efficiency of such an algorithm depends on the solution representation for each step. For bodies of relatively simple shape and some classes of boundary conditions, one can find analytic solutions generating efficient computational algorithms.

III. Analytic Solution at a Step

The solution for a single step is constructed under the assumption that the displacements and excess temperatures, as well as their gradients, are small. This allows one to

ISBN: 978-988-19253-5-0
ISSN: 2078-0958 (Print); ISSN: 2078-0966 (Online)

consider the problem for a step in the linear statement and to use the methods of expansion in biorthogonal systems of functions, which were developed in [8], [9].

The process of deformation is considered in the affine (point) space $\mathcal{E}$. From now on, the dot $(\cdot)$ denotes the inner product on $\mathcal{V}$. Up to negligibly small variables, the body configuration images $\mathfrak{B}$ can be identified with a parallelepiped V embedded in the space $\mathcal{E}$. The quantities $\hat{a}$, $\hat{b}$, $\hat{h}$ are the parallelepiped linear dimensions, which are assumed to be constant in a single step but can vary in the course of the accretion process.

Assume that a mass measure ρ is introduced on the body $\mathfrak{B}$, and the body is under the action of the external field of mass forces $\hat{\mathbf{K}}(\hat{\mathbf{r}})$ and of distributed heat sources whose specific capacity is determined by the field $\hat{\omega}(\hat{\mathbf{r}})$. The displacements $\hat{\mathbf{u}} = \hat{u}\mathbf{i} + \hat{v}\mathbf{j} + \hat{w}\mathbf{k}$ caused by these fields and their gradients are assumed to be negligibly small with respect to the coordinates of the points $\hat{\mathbf{r}}$ so that the latter are assumed to be constant, and the infinitesimal strain field $\varepsilon = \frac{1}{2}\left(\hat{\boldsymbol{\nabla}}\hat{\mathbf{u}} + (\hat{\boldsymbol{\nabla}}\hat{\mathbf{u}})^{\mathrm{T}}\right)$ is associated with the body $\mathfrak{B}$. Here $\hat{\boldsymbol{\nabla}} = \mathbf{i}\frac{\partial}{\partial\hat{x}} + \mathbf{j}\frac{\partial}{\partial\hat{y}} + \mathbf{k}\frac{\partial}{\partial\hat{z}}$ is the dimensional Hamiltonian operator, and $(\ldots)^{\mathrm{T}}$ is the transposition symbol.

The body response is determined by the linear Duhamel–Neumann functional [10] for the stresses $\hat{\boldsymbol{\sigma}}(\varepsilon, \hat{\theta})$

$$\hat{\boldsymbol{\sigma}}(\varepsilon, \hat{\theta}) = 2\mu\varepsilon + \lambda \boldsymbol{I} \otimes \boldsymbol{I} : \varepsilon - (3\lambda + 2\mu)\alpha\hat{\theta}\boldsymbol{I}$$

and by the linear Fourier functional determining the thermal flow $\hat{\mathbf{h}}(\hat{\theta})$ depending on the gradient of the excess temperature $\hat{\theta}$

$$\hat{\mathbf{h}} = -\Lambda\hat{\boldsymbol{\nabla}}\hat{\theta}. \tag{3}$$

Here μ and λ are the Lamé moduli for the adiabatic state, α is the coefficient of linear thermal expansion, Λ is the thermal conductivity coefficient, $\hat{\theta} = T - T_0$ is the excess temperature, T is the absolute temperature, and $T_0 = \mathrm{const}$ is the reading temperature.

Under the above assumptions, the coupled system of equations of motion and heat conduction has the form [10]:

$$\begin{cases} \mu\hat{\boldsymbol{\nabla}}^2\hat{\mathbf{u}} + (\lambda+\mu)\hat{\boldsymbol{\nabla}}\hat{\boldsymbol{\nabla}}\cdot\hat{\mathbf{u}} - (3\lambda+2\mu)\alpha\hat{\boldsymbol{\nabla}}\hat{\theta} - \rho\frac{\partial^2}{\partial\hat{t}^2}\hat{\mathbf{u}} + \rho\hat{\mathbf{K}} = \mathbf{0} \\ \Lambda\hat{\boldsymbol{\nabla}}^2\hat{\theta} - \rho c\frac{\partial}{\partial\hat{t}}\hat{\theta} - (3\lambda+2\mu)T_0\alpha\hat{\boldsymbol{\nabla}}\cdot\left(\frac{\partial}{\partial\hat{t}}\hat{\mathbf{u}}\right) + \rho\hat{\omega} = 0 \end{cases} \tag{4}$$

where c is the specific heat at constant deformation referred to unit mass and $\hat{\boldsymbol{\nabla}}^2 = \hat{\boldsymbol{\nabla}}\cdot\hat{\boldsymbol{\nabla}} = \frac{\partial^2}{\partial\hat{x}^2} + \frac{\partial^2}{\partial\hat{y}^2} + \frac{\partial^2}{\partial\hat{z}^2}$ is the dimensional Laplace operator. The fact that system (4) is coupled can be explained by the presence of the temperature gradient in the equations of motion and by the presence of the dilatation rate in the heat equation. In the literature, the coupled thermoelasticity of such a type is said to be "completely coupled." The equations of the so-called theory of temperatures stresses [10] do not take into account the dilatation rate influence on the process of heat conduction and represent "partially" coupled thermoelasticity. It was shown in [11] that taking into account the dilatation rate in heat equations leads to a significant correction of the solution for bodies of micron dimensions.

Consider the boundary conditions corresponding to the "smoothly rigid" heat-insulated fixation (In [12], exact solutions were investigated for an elastic parallelepiped with "sliding fixation.") on five of its faces Γ_1 and the free heat-insulated face Γ_2 (Fig. 1):

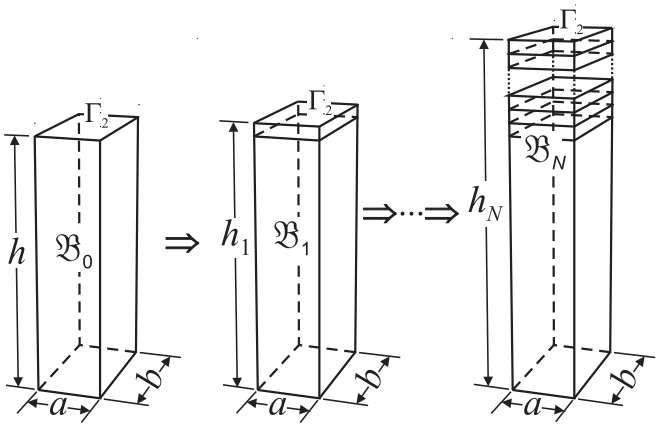

Fig. 1. The discrete process growing

$$\hat{\mathbf{u}}\cdot\mathbf{n}\big|_{\Gamma_1} = 0, \quad \mathbf{n}\cdot\hat{\boldsymbol{\sigma}}\cdot(\boldsymbol{I} - \mathbf{n}\otimes\mathbf{n})\big|_{\Gamma_1} = \mathbf{0}, \quad \hat{\mathbf{h}}\cdot\mathbf{n}\big|_{\Gamma_1} = 0,$$
$$\mathbf{n}\cdot\hat{\boldsymbol{\sigma}}\big|_{\Gamma_2} = \mathbf{0}, \quad \hat{\mathbf{h}}\cdot\mathbf{n}\big|_{\Gamma_2} = 0 \tag{5}$$

The initial conditions determine the distributions of the initial displacements $\hat{\mathbf{u}}_0$, the velocities $\hat{\mathbf{v}}_0$ and the excess temperature $\hat{\theta}_0$:

$$\hat{\mathbf{u}}\big|_{\hat{t}=0} = \hat{\mathbf{u}}_0, \quad \frac{\partial}{\partial\hat{t}}\hat{\mathbf{u}}_0\big|_{\hat{t}=0} = \hat{\mathbf{v}}_0, \quad \hat{\theta}\big|_{\hat{t}=0} = \hat{\theta}_0 \tag{6}$$

Relations (4)–(6) determine the mathematical statement of the problem for a single step.

When implementing the computational algorithm, it is expedient to pass to dimensionless spatial coordinates $\mathbf{r}$ referred to the characteristics dimension R and to the dimensionless time t which are related to the dimensional variables as follows:

$$\mathbf{r} = \frac{\hat{\mathbf{r}}}{R} = x\mathbf{i} + y\mathbf{j} + z\mathbf{k},\ x = \frac{\hat{x}}{R},\ y = \frac{\hat{y}}{R},\ z = \frac{\hat{z}}{R},\ t = \frac{\hat{t}}{R}\sqrt{\frac{\mu}{\rho}}.$$

The desired functions are the dimensionless displacements $\mathbf{u}$ and the dimensionless excess temperature θ referred to the reading temperature T_0,

$$\mathbf{u} = \frac{\hat{\mathbf{u}}}{R} = u\mathbf{i} + v\mathbf{j} + w\mathbf{k},\ u = \frac{\hat{u}}{R},\ v = \frac{\hat{v}}{R},\ w = \frac{\hat{w}}{R},\ \theta = \frac{\hat{\theta}}{T_0}.$$

Then the differentiation operations become

$$\boldsymbol{\nabla} = R\hat{\boldsymbol{\nabla}} = \mathbf{i}\frac{\partial}{\partial x} + \mathbf{j}\frac{\partial}{\partial y} + \mathbf{k}\frac{\partial}{\partial z},\ \boldsymbol{\nabla}^2 = R^2\hat{\boldsymbol{\nabla}}^2,\ \frac{\partial}{\partial t} = R\sqrt{\frac{\rho}{\mu}}\frac{\partial}{\partial\hat{t}}.$$

In the dimensionless variables, Eqs. (4) are reduced to the form

$$\begin{cases} \boldsymbol{\nabla}^2\mathbf{u} + A\boldsymbol{\nabla}\boldsymbol{\nabla}\cdot\mathbf{u} - B\boldsymbol{\nabla}\theta - \ddot{\mathbf{u}} + \mathbf{K} = \mathbf{0}, \\ \boldsymbol{\nabla}^2\theta - C\dot{\theta} - D\boldsymbol{\nabla}\cdot\dot{\mathbf{u}} + \omega = 0, \end{cases} \tag{7}$$

$$A = \frac{\lambda+\mu}{\mu}, \quad B = \frac{(3\lambda+2\mu)\alpha T_0}{\mu},$$
$$C = \frac{Rc\sqrt{\rho\mu}}{\Lambda}, \quad D = \frac{(3\lambda+2\mu)R\alpha\sqrt{\mu}}{\Lambda\sqrt{\rho}}.$$

In Eqs. (7) and later, the dot denotes the derivative $\frac{\partial}{\partial t}$, and the fields $\boldsymbol{K}$ and ω are the dimensionless densities of the force and thermal actions $\mathbf{K} = \frac{R\rho\hat{\mathbf{K}}}{\mu}$ and $\omega = \frac{R^2\rho\hat{\omega}}{\Lambda T}$.

ISBN: 978-988-19253-5-0
ISSN: 2078-0958 (Print); ISSN: 2078-0966 (Online)

The boundary and initial conditions (5)–(6) in the dimensionless variables are stated as

$$\begin{gathered}\mathbf{u}\cdot\mathbf{n}\otimes\mathbf{n}+\mathbf{n}\cdot\left(\boldsymbol{\nabla}\mathbf{u}+(\boldsymbol{\nabla}\mathbf{u})^{\mathrm{T}}\right)\cdot(\boldsymbol{I}-\mathbf{n}\otimes\mathbf{n})\big|_{\Gamma_1}=\mathbf{0},\\ \mathbf{n}\cdot\left(\boldsymbol{\nabla}\mathbf{u}+(\boldsymbol{\nabla}\mathbf{u})^{\mathrm{T}}\right)+\mathbf{n}\left((A-1)\boldsymbol{\nabla}\cdot\mathbf{u}-B\theta\right)\big|_{\Gamma_2}=\mathbf{0},\\ \mathbf{n}\cdot\boldsymbol{\nabla}\theta\big|_{\Gamma_1}=0,\quad \mathbf{n}\cdot\boldsymbol{\nabla}\theta\big|_{\Gamma_2}=0,\\ \mathbf{u}\big|_{t=0}=\mathbf{u}_0,\quad \dot{\mathbf{u}}\big|_{t=0}=\mathbf{v}_0,\quad \theta\big|_{t=0}=\theta_0,\end{gathered}\tag{8}$$

where $\mathbf{u}_0=\frac{\hat{\mathbf{u}}_0}{R}$, $\mathbf{v}_0=\hat{\mathbf{v}}_0\sqrt{\frac{\rho}{\mu}}$ and $\theta_0=\frac{\hat{\theta}_0}{T_0}$ are dimensionless initial data.

Equations (7) along with conditions (8) present the statement of the initial–boundary value problem in dimensionless form. The solution of this problem is sought as the spectral expansion according to [8], [9]. Since the differential operators generated by the system of Eqs. (7) are not self-adjoint, it is necessary to consider complex-valued functions, and hence it is necessary to introduce a Hilbert space $\mathcal{H}$ on the set of complex-valued vector functions

$$\mathbf{a}=\begin{pmatrix}\mathbf{u}\\ \theta\end{pmatrix}=\begin{pmatrix}u\mathbf{i}+v\mathbf{j}+w\mathbf{k}\\ \theta\end{pmatrix}$$

defined and square integrable in the domain V and satisfying the condition that the bilinear form determining the inner product $\langle\cdot,\cdot\rangle$ in $\mathcal{H}$ is meaningful,

$$\forall\mathbf{a},\mathbf{b}\in\mathcal{H}:\ \langle\mathbf{a},\mathbf{b}\rangle=\left\langle\begin{pmatrix}\mathbf{u},\\ \theta,\end{pmatrix}\begin{pmatrix}\mathbf{v},\\ \xi\end{pmatrix}\right\rangle=\int_V\left(\mathbf{u}\cdot\bar{\mathbf{v}}+\theta\bar{\xi}\right)\,dV.$$

Here the bar denotes complex conjugation.

The coupled equations of motion and heat conduction (7) along with the boundary conditions (8) determine a pencil of differential operators in $\mathcal{H}$, which can be written in matrix form

$$\mathcal{L}_\nu=\begin{pmatrix}\boldsymbol{\nabla}^2-\nu^2\boldsymbol{I}+A\boldsymbol{\nabla}\boldsymbol{\nabla}\cdot & -B\boldsymbol{\nabla}\\ -D\nu\boldsymbol{\nabla}\cdot & \boldsymbol{\nabla}^2-C\nu\end{pmatrix}.$$

The domain of the operator $\mathcal{L}_\nu$ is denoted by the symbol $\mathcal{D}$ and is defined as a subset of $\mathcal{H}$:

$$\begin{gathered}\mathcal{D}=\left\{\mathbf{a}\mid\mathcal{B}_1\mathbf{a}=\mathbf{0}\wedge\mathcal{B}_2\mathbf{a}=\mathbf{0}\right\}\subset\mathcal{H},\\ \mathcal{B}_1\begin{pmatrix}\mathbf{u}\\ \theta\end{pmatrix}=\begin{pmatrix}\mathbf{u}\mathbf{n}\otimes\mathbf{n}+\mathbf{n}\cdot\left(\boldsymbol{\nabla}\mathbf{u}+(\boldsymbol{\nabla}\mathbf{u})^{\mathrm{T}}\right)\cdot(\boldsymbol{I}-\mathbf{n}\otimes\mathbf{n})\big|_{\Gamma_1}\\ \mathbf{n}\cdot\boldsymbol{\nabla}\theta\big|_{\Gamma_1}\end{pmatrix},\\ \mathcal{B}_2\begin{pmatrix}\mathbf{u}\\ \theta\end{pmatrix}=\begin{pmatrix}\mathbf{n}\cdot\left(\boldsymbol{\nabla}\mathbf{u}+(\boldsymbol{\nabla}\mathbf{u})^{\mathrm{T}}\right)+\mathbf{n}\left((A-1)\boldsymbol{\nabla}\cdot\mathbf{u}-B\theta\right)\big|_{\Gamma_2}\\ \mathbf{n}\cdot\boldsymbol{\nabla}\theta\big|_{\Gamma_2}\end{pmatrix},\end{gathered}$$

where $\mathcal{B}_1$ and $\mathcal{B}_2$ are the operators of boundary conditions.

The operator pencil $\mathcal{L}_\nu$ is associated with the adjoint pencil $\mathcal{L}_\nu^*$ defined in the domain $\mathcal{D}^*\subset\mathcal{H}$ and satisfying the following relations:

$$\forall\mathbf{u}\in\mathcal{D},\quad\forall\mathbf{v}\in D^*\quad\langle\mathcal{L}_\nu\mathbf{u},\mathbf{v}\rangle=\langle\mathbf{u},\mathcal{L}_\nu^*\mathbf{v}\rangle.$$

The adjoint pencil can be defined explicitly as [8]

$$\begin{gathered}\mathcal{L}_\nu^*=\begin{pmatrix}\boldsymbol{\nabla}^2-\bar{\nu}^2\boldsymbol{I}+A\boldsymbol{\nabla}\boldsymbol{\nabla}\cdot & D\bar{\nu}\boldsymbol{\nabla}\\ B\boldsymbol{\nabla}\cdot & \boldsymbol{\nabla}^2-C\bar{\nu}\end{pmatrix},\\ \mathcal{D}^*=\left\{\mathbf{a}\mid\mathcal{B}_1^*\mathbf{a}=\mathbf{0}\wedge\mathcal{B}_2^*\mathbf{a}=\mathbf{0}\right\}\subset\mathcal{H},\\ \mathcal{B}_1^*=\mathcal{B}_1,\\ \mathcal{B}_2^*\begin{pmatrix}\mathbf{u}\\ \theta\end{pmatrix}=\begin{pmatrix}\mathbf{n}\cdot(\boldsymbol{\nabla}\mathbf{u}+(\boldsymbol{\nabla}\mathbf{u})^*)+\mathbf{n}\left((A-1)\boldsymbol{\nabla}\cdot\mathbf{u}+\bar{\nu}D\theta\right)\big|_{\Gamma_2}\\ \mathbf{n}\cdot\boldsymbol{\nabla}\theta\big|_{\Gamma_2}\end{pmatrix}.\end{gathered}$$

The pair of mutually adjoint operators $\mathcal{L}_\nu$ and $\mathcal{L}_\nu^*$ generates mutually adjoint eigenvalue problems (generalized Sturm–Liouville problems)

$$\mathcal{L}_\nu\mathbf{k}=\mathbf{0},\quad\mathcal{L}_\nu^*\mathbf{k}^*=\mathbf{0}.\tag{9}$$

Since the domain V is bounded and the differential operator under study are regular, the nontrivial solutions of problems (9) form countable sequences of complex-valued vector functions $\{\mathbf{k}_i\}$, $\{\mathbf{k}_i^*\}$, $i=1,2,\ldots$, which correspond to the sequence of generalized eigenvalues $\{\nu_i\}$. Since the operator pencils are not self-adjoint, the eigenvalues are generally located on the complex plane in a rather complicated way, but since the coefficient D is positive and small, one can show that the eigenvalues form three subsequences one of which consists of numbers on the negative real semiaxis and has the limit point $-\infty$, and the other two sequences are located near the imaginary axis in the negative half-plane and have the accumulation points $\pm i\infty$. The same reasoning shows that the function systems $\{\mathbf{k}_i\}$ and $\{\mathbf{k}_i^*\}$ are complete in $\mathcal{H}$.Moreover, the functions $\mathbf{k}_i$ and $\mathbf{k}_j^*$ $i\neq j$ satisfy the biorthogonality conditions [8]:

$$\begin{gathered}\left\langle\mathcal{H}_1\mathbf{k}_i,\mathbf{k}_j^*\right\rangle+(\nu_i+\nu_j)\left\langle\mathcal{H}_2\mathbf{k}_i,\mathbf{k}_j^*\right\rangle=0,\\ \mathcal{H}_1=\begin{pmatrix}\mathbf{0} & 0\\ -D\boldsymbol{\nabla}\cdot & -C\end{pmatrix},\quad\mathcal{H}_2=\begin{pmatrix}-\boldsymbol{I} & 0\\ \mathbf{0} & 0\end{pmatrix},\end{gathered}$$

which can explicitly be written as

$$-\int_V\left[(D\boldsymbol{\nabla}\cdot\mathbf{u}_i+C\theta_i)\,\bar{\theta}_j^*+(\nu_i+\nu_j)\mathbf{u}_i\cdot\bar{\mathbf{u}}_j^*\right]\,dV=0,$$

$$\mathbf{k}_i=\begin{pmatrix}\mathbf{u}_i\\ \theta_i\end{pmatrix},\quad\mathbf{k}_j^*=\begin{pmatrix}\mathbf{u}_j^*\\ \theta_j^*\end{pmatrix}.$$

Thus, the function systems $\{\mathbf{k}_i\}$ and $\{\mathbf{k}_i^*\}$ form mutually biorthogonal bases in $\mathcal{H}$. According to [8], the solution of the initial–boundary value problem (7), (8) can be represented by the expansion

$$\begin{gathered}\begin{pmatrix}\mathbf{u}\\ \theta\end{pmatrix}=\sum_{i=1}^{\infty}\left[\left\langle\left\langle\begin{pmatrix}\mathbf{u}_0\\ \theta_0\end{pmatrix},\mathcal{H}_1^*\mathbf{k}_i^*+\bar{\nu}_i\mathcal{H}_2\mathbf{k}_i^*\right\rangle\right.\right.\\ \left.\left.+\left\langle\begin{pmatrix}\mathbf{v}_0\\ 0\end{pmatrix},\mathcal{H}_2\mathbf{k}_i^*\right\rangle\right)e^{\nu t}-\int_0^t\left\langle\begin{pmatrix}\mathbf{K}\\ \omega\end{pmatrix},\mathbf{k}_i^*\right\rangle e^{\nu_i(t-\tau)}\Bigg]\mathbf{k}_i N_i^{-1},\\ \mathcal{H}_1^*=\begin{pmatrix}\mathbf{0} & D\boldsymbol{\nabla}\cdot\\ \mathbf{0} & -C\end{pmatrix},\end{gathered}\tag{10}$$

where $N_i=\langle\mathcal{H}_1\mathbf{k}_i,\mathbf{k}_i^*\rangle+2\nu_i\langle\mathcal{H}_2\mathbf{k}_i,\mathbf{k}_i^*\rangle$ are the normalizing factors.

The efficiency of representation (10) depends on the efficiency of the representation of the functions $\{\mathbf{k}_i\}$ and $\{\mathbf{k}_i^*\}$, i.e., on the solutions of the generalized Sturm–Liouville problems [11]. As a rule, these solutions for three-dimensional problems either cannot at all be written in closed form or their representations ar extremely cumbersome. At the same time, the problem considered in this paper admits a very compact representations of all components of the expansion (also see [12]).

IV. Account the Relaxing of the Heat Flux

One of the drawbacks of the classical law (3) is the fact that the thermal signal transmission speed turns out to be infinite in applications. Nevertheless, it effectively describes heat propagation in a wide range of applications. Therefore,

ISBN: 978-988-19253-5-0
ISSN: 2078-0958 (Print); ISSN: 2078-0966 (Online)

the Fourier law has to be modified only if the relaxation time and the external action pulse duration are quantities of the same order of magnitude.

In the last two hundred years, various linear generalizations of the Fourier heat conduction law have been suggested (a survey and historic comments are given in [13]). In the literature, most frequently used is the Cattaneo–Jeffreys law, which can be written as

$$\tau_1\dot{\mathbf{h}} + \mathbf{h} = -\Lambda\boldsymbol{\nabla}\theta, \tag{11}$$

where τ_1 is the relaxation time.

In the present paper, we use the heat conduction law with two relaxation times τ_1 and τ_2, namely,

$$\tau_1\dot{\mathbf{h}} + \mathbf{h} = -\Lambda(\boldsymbol{\nabla}\theta + \tau_2\boldsymbol{\nabla}\dot{\theta}). \tag{12}$$

The choice of the law in the form (12) is a natural generalization of coupling laws in differential form. Here it is appropriate to draw an analogy with, for example, the constitutive relations of linear viscoelasticity in differential form.

Now let us reformulate the statement of the problem. The heat conduction equation in system (4) has to be replaced by the following one

$$\Lambda(\boldsymbol{\nabla}^2\theta + \tau_2\boldsymbol{\nabla}^2\dot{\theta}) - \rho c(\tau_1\ddot{\theta} + \dot{\theta}) - (3\lambda + 2\mu)\alpha\theta_0(\tau_1\boldsymbol{\nabla}\cdot\ddot{\mathbf{u}} + \boldsymbol{\nabla}\cdot\dot{\mathbf{u}}) + \tau_1\dot{\omega} + \omega = 0. \tag{13}$$

The boundary conditions, corresponding to heat conduction, may be formulated as

$$[C(\tau_1\dot{\theta} + \theta) - D\Lambda\mathbf{n}\cdot(\tau_2\boldsymbol{\nabla}\dot{\theta} + \boldsymbol{\nabla}\theta)]\big|_{\partial V} = 0.$$

The initial temperature rate distribution ϑ^0 should be specified as the initial data:

$$\dot{\theta}\big|_{t=0} = \vartheta^0. \tag{14}$$

In dimensionless variables the mention above equations have the following form

$$\tilde{\boldsymbol{\nabla}}^2\tilde{\theta} + E\frac{\partial}{\partial\tilde{t}}\tilde{\boldsymbol{\nabla}}^2\tilde{\theta} - F\frac{\partial^2\tilde{\theta}}{\partial\tilde{t}^2} - C\frac{\partial\tilde{\theta}}{\partial\tilde{t}} - G\frac{\partial^2}{\partial\tilde{t}^2}\tilde{\boldsymbol{\nabla}}\cdot\tilde{\mathbf{u}} - D\tilde{\boldsymbol{\nabla}}\cdot\frac{\partial\tilde{\mathbf{u}}}{\partial\tilde{t}} + \tilde{\Omega}_1 = 0. \tag{15}$$

The coefficients E, F, G can be written as

$$E = \frac{\tau_2\sqrt{\mu}}{R\sqrt{\rho}}, \quad F = \frac{\tau_1 c\mu}{\Lambda}, \quad G = \frac{\tau_1(3\lambda + 2\mu)\alpha\mu}{\rho\Lambda}.$$

The dimensionless inhomogeneous terms can be calculated by the formulas

$$\tilde{\Omega} = \frac{R^2}{\Lambda\theta_0}\omega, \quad \tilde{\Omega}_1 = \frac{R^2}{\Lambda\theta_0}(\tau_1\dot{\omega} + \omega).$$

The boundary conditions have the dimensionless form

$$\left(\tilde{E}\frac{\partial}{\partial\tilde{t}}\tilde{\theta} + \tilde{C}\tilde{\theta} - \tilde{F}\frac{\partial}{\partial\tilde{t}}\mathbf{n}\cdot\tilde{\boldsymbol{\nabla}}\tilde{\theta} - \tilde{D}\tilde{\boldsymbol{\nabla}}\mathbf{n}\cdot\tilde{\boldsymbol{\nabla}}\tilde{\theta}\right)\Big|_{\partial V} = 0, \quad \tilde{E} = C\frac{\tau_1}{\Lambda R}\sqrt{\frac{\mu}{\rho}}, \quad \tilde{F} = D\frac{\tau_2}{R^2}\sqrt{\frac{\mu}{\rho}}. \tag{16}$$

The initial data in dimensionless form are formulated as

$$\tilde{\theta}\big|_{\tilde{t}=0} = \frac{\theta^0}{\theta_0}, \quad \dot{\tilde{\theta}}\big|_{\tilde{t}=0} = \vartheta^0\frac{R}{\theta_0}\sqrt{\frac{\rho}{\mu}}.$$

The initial-boundary problems used in the present paper generate quadratic pencils of the form

$$\boldsymbol{\mathcal{L}}_\nu = \boldsymbol{\mathcal{H}}_0 + \nu\boldsymbol{\mathcal{H}}_1 + \nu^2\boldsymbol{\mathcal{H}}_2.$$

The operator coefficients are formulated as

$$\boldsymbol{\mathcal{H}}_0 = \begin{pmatrix} \tilde{\boldsymbol{\nabla}}^2 + A\tilde{\boldsymbol{\nabla}}\otimes\tilde{\boldsymbol{\nabla}}\cdot & -B\tilde{\boldsymbol{\nabla}} \\ \mathbf{0} & \tilde{\boldsymbol{\nabla}}^2 \end{pmatrix},$$

$$\boldsymbol{H}_1 = \begin{pmatrix} \mathbf{0} & 0 \\ -D\tilde{\boldsymbol{\nabla}}\cdot & E\tilde{\boldsymbol{\nabla}}^2 - C \end{pmatrix}, \quad \boldsymbol{\mathcal{H}}_2 = \begin{pmatrix} -\mathbf{E} & 0 \\ -G\tilde{\boldsymbol{\nabla}}\cdot & -F \end{pmatrix}.$$

We recall that the differential operators $\boldsymbol{\mathcal{H}}_0$, $\boldsymbol{\mathcal{H}}_1$, and $\boldsymbol{\mathcal{H}}_2$ have a common domain of definition $\boldsymbol{\mathcal{D}}_{\boldsymbol{\mathcal{H}}}$ determined by the boundary condition operator $\boldsymbol{\mathcal{B}}_{\boldsymbol{\mathcal{H}}}$:

$$\boldsymbol{\mathcal{B}}_{\boldsymbol{\mathcal{H}}}\begin{pmatrix}\mathbf{u}\\ \theta\end{pmatrix} = \begin{pmatrix} [\tilde{\boldsymbol{\nabla}}\mathbf{u} + (\tilde{\boldsymbol{\nabla}}\mathbf{u})^*]\cdot\mathbf{n} + \mathbf{n}(A-1)\tilde{\boldsymbol{\nabla}}\cdot\mathbf{u} - B\theta \\ \tilde{E}\nu\theta + \tilde{C}\theta - \tilde{F}\nu\mathbf{n}\cdot\tilde{\boldsymbol{\nabla}}\theta - D\mathbf{n}\cdot\tilde{\boldsymbol{\nabla}}\theta \end{pmatrix}\Big|_{\partial V}.$$

For the initial-boundary problem under study, the adjoint pencil has the form

$$\boldsymbol{\mathcal{L}}^*_{\upsilon} = \boldsymbol{\mathcal{H}}^*_0 + \bar{\upsilon}\boldsymbol{\mathcal{H}}^*_1 + \bar{\upsilon}^2\boldsymbol{\mathcal{H}}^*_2,$$

$$\boldsymbol{\mathcal{H}}^*_1 = \begin{pmatrix} \mathbf{0} & D\tilde{\boldsymbol{\nabla}} \\ \mathbf{0} & E\tilde{\boldsymbol{\nabla}}^2 - C \end{pmatrix}, \quad \boldsymbol{\mathcal{H}}^*_2 = \begin{pmatrix} \mathbf{E} & G\tilde{\boldsymbol{\nabla}} \\ \mathbf{0} & -F \end{pmatrix}.$$

The domain of definition of the adjoint pencil

$$\boldsymbol{\mathcal{D}}^*_{\boldsymbol{\mathcal{H}}} = \{\mathbf{y} \mid \boldsymbol{\mathcal{B}}^*_{\boldsymbol{\mathcal{H}}}[\mathbf{y}] = \mathbf{0}\},$$

$$\boldsymbol{\mathcal{B}}^*_{\boldsymbol{\mathcal{H}}}\begin{pmatrix}\mathbf{u}\\ \theta\end{pmatrix} = \begin{pmatrix} [\tilde{\boldsymbol{\nabla}}\mathbf{u} + (\tilde{\boldsymbol{\nabla}}\mathbf{u})^*]\cdot\mathbf{n} + \mathbf{n}(A-1)\tilde{\boldsymbol{\nabla}}\cdot\mathbf{u} + \bar{\upsilon}D\theta \\ \tilde{E}\bar{\upsilon}\theta + \tilde{C}\theta - \tilde{F}\bar{\upsilon}\mathbf{n}\cdot\tilde{\boldsymbol{\nabla}}\theta + \tilde{B}\mathbf{n}\cdot\tilde{\boldsymbol{\nabla}}\theta \end{pmatrix}\Big|_{\partial V}.$$

V. Representations of the Eigenfunctions

Let us focus on system (4). The representation of functions of the family $\{\mathbf{k}_i\}$ (and respectively, of $\{\mathbf{k}^*_i\}$) which is consistent with the boundary conditions (8) has the form

$$\mathbf{k} = \begin{pmatrix} \mathbf{i}\sin(nx)\,\cos(my)\,a(z) + \mathbf{j}\cos(nx)\,\sin(my)\,b(z) \\ +\mathbf{k}\cos(nx)\,\cos(my)\,c(z) \\ \cos(nx)\,\cos(my)\,d(z) \end{pmatrix},$$

where, for brevity, the following notation is used: $n = \frac{n'\pi}{a}$, $m = \frac{m'\pi}{b}$, n', $m' \in \mathbb{N}$, and $\mathbb{N}$ is the set of positive integers; the functions $a(z)$, $b(z)$, $c(z)$, and $d(z)$ are determined by solving the system of linear differential equations

$$\begin{pmatrix} 1 & 0 & 0 & 0 \\ 0 & 1 & 0 & 0 \\ 0 & 0 & 1+A & 0 \\ 0 & 0 & 0 & 1 \end{pmatrix}.\vec{U}'' + \begin{pmatrix} 0 & 0 & -An & 0 \\ 0 & 0 & -Am & 0 \\ An & Am & 0 & -B \\ 0 & 0 & -D\nu & 0 \end{pmatrix}.\vec{U}' - \begin{pmatrix} (1+A)n^2 + m^2 + \nu^2 & Amn & 0 & -Bn \\ Amn & (1+A)m^2 + n^2 + \nu^2 & 0 & -Bm \\ 0 & 0 & n^2+m^2+\nu^2 & 0 \\ D\nu n & D\nu m & 0 & n^2+m^2+C\nu \end{pmatrix}.\vec{U} = \vec{0} \tag{17}$$

Here $\vec{U} = (a(z), b(z), c(z), d(z))^{\mathrm{T}}$ is a formal four-component vector function, and the prime $'$ denotes the derivatives with respect to the variable z. Note that system (17) is not symmetric, because the initial problem is not self-adjoint.

ISBN: 978-988-19253-5-0
ISSN: 2078-0958 (Print); ISSN: 2078-0966 (Online)

Although the order of the system of Eqs. (17) is rather high, the fundamental system of its solutions has the simple form

$$\vec{U}_1=\begin{pmatrix}-m\\ n\\ 0\\ 0\end{pmatrix}e^{\zeta z},\quad \vec{U}_2=\begin{pmatrix}-m\\ n\\ 0\\ 0\end{pmatrix}e^{-\zeta z},\quad \vec{U}_3=\begin{pmatrix}-\zeta\\ 0\\ n\\ 0\end{pmatrix}e^{\zeta z},$$

$$\vec{U}_4=\begin{pmatrix}\zeta\\ 0\\ n\\ 0\end{pmatrix}e^{-\zeta z},\quad \vec{U}_5=\begin{pmatrix}m\\ n\\ -\xi\\ \frac{2D\nu^2}{P}\end{pmatrix}e^{\xi z},\quad \vec{U}_6=\begin{pmatrix}m\\ n\\ \xi\\ \frac{2D\nu^2}{P}\end{pmatrix}e^{-\xi z},$$

$$\vec{U}_7=\begin{pmatrix}m\\ n\\ -\eta\\ \frac{2D\nu^2}{Q}\end{pmatrix}e^{\eta z},\quad \vec{U}_8=\begin{pmatrix}m\\ n\\ \eta\\ \frac{2D\nu^2}{Q}\end{pmatrix}e^{-\eta z},$$

$$\zeta=\sqrt{\nu^2+n^2+m^2},\quad \xi=\sqrt{n^2+m^2+\nu\frac{Q+2\nu}{2(A+1)}},$$

$$\eta=\sqrt{n^2+m^2+\nu\frac{P+2\nu}{2(A+1)}},\quad P=R+\sqrt{R^2+M},$$

$$Q=R-\sqrt{R^2+M},\quad R=AC+BD+C-\nu,\quad M=4\nu BD.$$

By substituting the fundamental solutions into the boundary conditions corresponding to the upper and lower faces of the parallelepiped ($z=0,h$), one obtains a system of eight linear equations for the constants of integration of system (17). By equating the determinant of the coefficients of this system with zero, one obtains an equation for the eigenvalues ν_i. This determinant can be written in the very concise form

$$\begin{aligned}&\left[e^{2\zeta h}-1\right]\Big[P^2\eta L^2\sinh(\zeta h)\cosh(\xi h)\sinh(\eta h)\\ &\quad+M\xi L^2\sinh(\zeta h)\sinh(\xi h)\cosh(\eta h)\\ &-2\zeta\xi\eta\left(L-\nu^2\right)\left(P^2+M\right)\cosh(\zeta h)\sinh(\xi h)\sinh(\eta h)\Big]=0,\end{aligned}\tag{18}$$

where $L=\nu^2+2(n^2+m^2)$.

The eigenfunctions can be classified by expanding the left-hand side of Eq. (18). The first class consists of the eigenfunctions associated with the zeros of the first factor on the right-hand side in Eq. (18); i.e.,

$$e^{2\zeta h}-1=0\quad\Rightarrow\quad 2\zeta h=2\pi ik,\quad k=1,2,\ldots.$$

The corresponding eigenvalues can be written as

$$\nu^{(I)}_{nmk}=i\sqrt{n^2+m^2+\left(\frac{k\pi}{h}\right)^2},\quad n,m,k\in\mathbb{N},$$

and the corresponding eigenfunctions have the form

$$\mathbf{k}^{(I)}_{nmk}=\begin{pmatrix}-\mathbf{i}\,m\sin(nx)\cos(my)\cos\left(\frac{k\pi z}{h}\right)\\ +\mathbf{j}\,n\sin(nx)\cos(my)\cos\left(\frac{k\pi z}{h}\right)\\ 0\end{pmatrix}.\tag{19}$$

The eigenfunctions of the second class determine the coupled thermoelastic vibrations. The corresponding eigenvalues can be determined as complex-values roots of the transcendental equation

$$\begin{aligned}&P^2\eta L^2\sinh(\zeta h)\cosh(\xi h)\sinh(\eta h)\\ &\quad+M\xi L^2\sinh(\zeta h)\sinh(\xi h)\cosh(\eta h)\\ &-2\zeta\xi\eta\left(L-\nu^2\right)\left(P^2+M\right)\cosh(\zeta h)\sinh(\xi h)\sinh(\eta h)=0\end{aligned}\tag{20}$$

and for the initial approximations one can take the real roots of the equation of uncoupled heat conduction and the pure imaginary roots of the equation for elastic vibrations, which are determined by the equations

$$\sinh(\eta h)=0,$$
$$L^2\sinh(\zeta h)\cosh(\xi h)-2\zeta\xi\left(L-\nu^2\right)\cosh(\zeta h)\sinh(\xi h)=0.$$

Note that for $n=m=0$ and $L=\nu^2$, the right-hand side of Eq. (20) splits into the factors

$$\begin{aligned}&\sinh(\zeta h)\left[P^2\eta\cosh(\xi h)\sinh(\eta h)+\right.\\ &\qquad\left.+M\xi\sinh(\zeta h)\sinh(\xi h)\cosh(\eta h)\right]=0\end{aligned}\tag{21}$$

The roots of Eqs. (20)–(21) are associated with the complex-valued eigenfunctions, and they can be written in the following common general form:

$$\mathbf{k}^{(II)}_{nmk}=\begin{pmatrix}\mathbf{i}\,n\Big[Y\zeta\cosh(\zeta z)+W\cosh(\xi z)\\ \quad-V\cosh(\eta z)\Big]\sin(nx)\cos(my)\\ \quad+\mathbf{j}\,m\Big[Y\zeta\cosh(\zeta z)+W\cosh(\xi z)\\ \quad-V\cosh(\eta z)\Big]\cos(nx)\sin(my)\\ \quad+\mathbf{k}\Big[\eta V\sinh(\eta z)-Y(n^2+m^2)\sinh(\zeta z)\\ \quad-\xi W\sinh(\xi z)\Big]\cos(nx)\cos(my)\\ 2D\nu^2\left[\frac{W}{P}\cosh(\xi z)-\frac{V}{Q}\cosh(\eta z)\right]\cos(nx)\cos(ny)\end{pmatrix},$$

$$\begin{aligned}Y&=2L\left[\xi\sinh(h\xi)\cosh(h\eta)-\eta\cosh(h\xi)\sinh(h\eta)\right],\\ V&=4[n^2+m^2]\zeta\xi\sinh(h\xi)\cosh(h\zeta)-L^2\cosh(h\xi)\sinh(h\zeta),\\ W&=4[n^2+m^2]\zeta\eta\sinh(h\eta)\cosh(h\zeta)-L^2\cosh(h\eta)\sinh(h\zeta).\end{aligned}$$

The representation of the eigenfunctions in the case heat conduction law (12) has the same structure.

VI. Numerical Simulation

As was already noted, the effects of coupled mechanical and thermal fields play a significant role for bodies of micron dimensions. Therefore, it is of special interest to model the process of thermoelastic accretion for bodies of such scales.

Consider the thermoelastic process of growth of a microscopic copper crystal which is represented as a growing parallelepiped with the initial dimensions $\hat{a}=R$, $\hat{b}=2R$, and $\hat{h}=4R$. Here R is the characteristic dimension equal to $1\,\mu$m (i.e., $R=10^{-6}$ m). The numerical simulation is based on the following physical and mechanical characteristics: $\lambda=89.4708$ GPa, $\mu=40.9531$ GPa, $\rho=8960$ kg/m^3, $\alpha=16.4\cdot10^{-6}$ 1/K, $\Lambda=385$ W/(m·K), and $c=385$ J/(kg·K).

Consider the "fast" accretion process. It is assumed that the growth is uniform, i.e., $\Delta h=h_{k+1}-h_k=\text{const}$ and $\Delta\tau=\tau_{k+1}-\tau_k=\text{const}$. The dimensionless rate of the material attachment is $v_a=\frac{\Delta h}{\Delta\tau}=0.1$, which corresponds to the dimensional rate $\hat{v}_a=213$ m/s. This rate value is associated with the characteristic time the growing body height doubling $\hat{\tau}_a=18.71$ ns. Note that τ_a is approximately five times greater than the period of the fundamental mode of the body vibrations at the beginning of the accretion process (3.658 ns) and is five times less than the basic relaxation time (91.27 ns), i.e., the value inverse to the real eigenvalue that is the least in absolute value. The given rate value $\hat{v}_a$ is associated with different accretion scenarios corresponding to different Δh. There is an analogy with different partitions

ISBN: 978-988-19253-5-0
ISSN: 2078-0958 (Print); ISSN: 2078-0966 (Online)

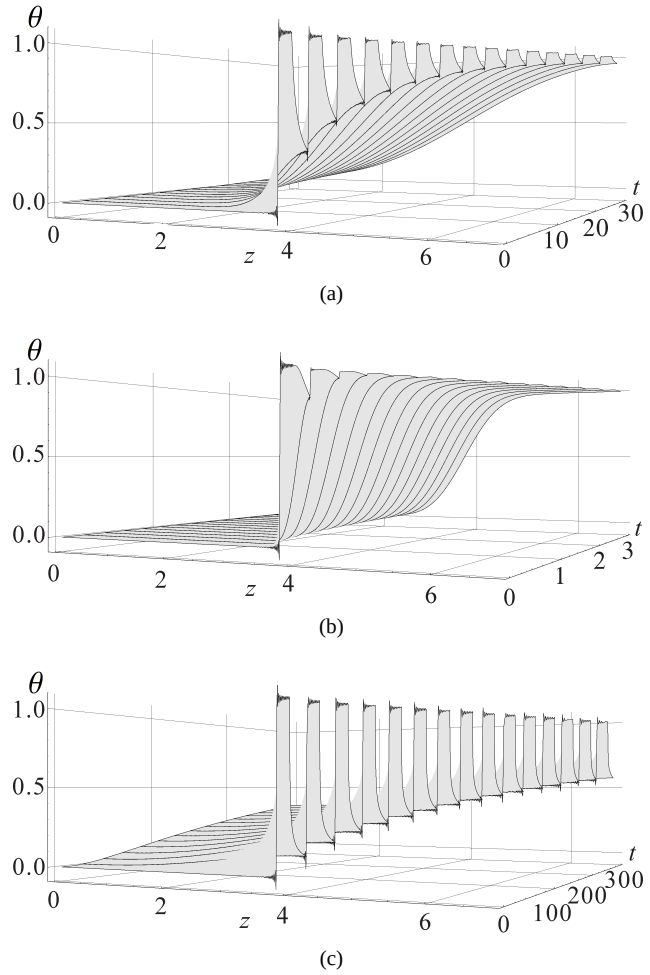

Fig. 2. The dependence of the temperature for the different rate of growth: (a) v_a, (b) $10v_a$, (c) $0.1v_a$

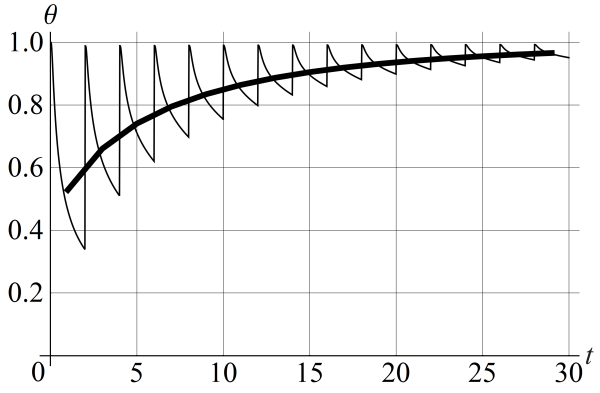

Fig. 3. The temperature on the moving boundary (thin line) and its value averaged over the step (thick line)

in the theory of integration. A decrease in Δh leads to a decrease in $\Delta\tau = \frac{\Delta h}{v_a}$, and the process of discrete accretion approaches a continuous process. Therefore, the numerical simulation of such a limit process is of great interest.

For further computations, it is assumed that the excess dimensionless temperature of the attached body $\mathfrak{B}_{k+1}\setminus\mathfrak{B}_k$ is equal to $\theta\big|_{t=\tau_k} = 1$, and the excess temperature of the body at the beginning of the growth $\mathfrak{B}_0$ is equal to $\theta\big|_{t=0} = 0$.

It is also assumed that there are no mass forces $\hat{\mathbf{K}}$ and no internal heat sources $\hat{\omega}$, and at the initial time moment, the growing body was free from stresses and at rest. The computational algorithm implementation according to the solution representation constructed in the paper allows one to determine the stresses, temperature, and velocities of points of the discretely built-up body at any time moment.

Figure 2 *a* shows the dependence of the temperature θ at the middle points of the parallelepiped cross-sections ($x = \frac{a}{2}$, $y = \frac{b}{2}$) on the coordinate z and time t, which corresponds to the accretion scenario with successively attached 15 layers ($N = 15$) of dimensionless thickness $\Delta h = 0.2$ ($\Delta\hat{h} = 0.2\,\mu$m). For the accepted accretion rate $v_a = 0.1$, one has the quantity $\Delta\tau = \frac{\Delta h}{v_a} = 2$ ($\Delta\hat{\tau} = 0.09355$ ns), and the parallelepiped height increases from $\hat{h} = 4\,\mu$m to $\hat{h}_{15} = 7\,\mu$m. For these parameters, the accretion process has the same typical time parameters as the heat transfer process. In particular, this is illustrated by the graph; namely, the temperature on the growth boundary smoothly varies from the initial temperature of the body to the temperature of the attached layers. Figure 2 *b* illustrates the temperature distribution for the rate of growth that is ten times greater than v_a. The effective (step-averaged) temperature of the growing boundary is close to the temperature of the attached layers. Figure 2 *c* shows the temperature distribution for the rate of growth that is ten times less that v_a. Figure 3 shows the temperature on the moving boundary (thin line) and its value averaged over the step (thick line).

An analysis of the temperature behavior on the growth boundary shows that, depending on the accretion rate, the boundary can be considered as an isothermal (for high values of the accretion rate) boundary or a boundary with variable "effective" temperature determined in the process of solving the problem.

References

[1] N. K. Arutyunyan, A. V. Manzhirov, and V. E. Naumov, *Contact Problems in Mechanics of Growing Solids*. Moscow: Nauka, 1991, [in Russian].

[2] A. V. Manzhirov, "The general non-inertial initial-boundaryvalue problem for a viscoelastic ageing solid with piecewise-continuous accretion," *J. Appl. Math. Mech.*, vol. 59, no. 5, pp. 805–816, 1995.

[3] A. V. Manzhirov and D. A. Parshin, "Accretion of a viscoelastic ball in a centrally symmetric force field," *Mech. Solids.*, vol. 41, no. 1, pp. 51–64, 2006.

[4] S. A. Lychev, T. N. Lycheva, and A. V. Manzhirov, "Unsteady vibration of a growing circular plate," *Mech. Solids*, vol. 46, no. 2, pp. 325–333, 2011.

[5] S. I. Kuznetsov, A. V. Manzhirov, and I. Fedotov, "Heat conduction problem for a growing ball," *Mech. Solids*, vol. 46, no. 6, pp. 929–936, 2011.

[6] A. V. Manzhirov and S. A. Lychev, "The mathematical theory of growing solids: Finite deformations," *Dokl. Phys.*, vol. 57, no. 4, pp. 160–163, 2012.

[7] A. L. Levitin, S. A. Lychev, A. V. Manzhirov, and M. Y. Shatalov, "Nonstationary vibrations of a discretely accreted thermoelastic parallelepiped," *Mech. Solids*, vol. 47, no. 6, pp. 677–689, 2012.

[8] S. A. Lychev and Y. E. Senitskii, "Nonsymmetric finite integral transformations and their applications to viscoelasticity problems," *Vestnik Samar. Gos. Univ. Estestvennonauchn. Ser.*, vol. Special Issue, pp. 16–38, 2002, [in Russian].

[9] S. A. Lychev, "Coupled dynamic thermoviscoelasticity problem," *Mech. Solids*, vol. 43, no. 5, pp. 769–784, 2008.

[10] W. Nowacki, *Theory of Elasticity*. Warsaw: PWN, 1970.

[11] S. A. Lychev, A. V. Manzhirov, and S. V. Joubert, "Closed solutions of boundary-value problems of coupled thermoelasticity," *Mech. Solids*, vol. 45, no. 4, pp. 610–623, 2010.

[12] P. A. Zhilin and T. P. Il'icheva, "Spectra and oscillation mode shapes of a rectangular parallelepiped obtained using three-dimensional theory of elasticity and theory of plates," *Mech. Solids*, vol. 15, no. 2, pp. 94–103, 1980.

[13] D. D. Joseph and L. Preziosi, "Heat waves," *Mod. Phys.*, vol. 61, no. 1, pp. 41–73, 1989.

ISBN: 978-988-19253-5-0
ISSN: 2078-0958 (Print); ISSN: 2078-0966 (Online)